Efficient Hybrid Method for Pan-Sharpening Enhancement of Multiband Satellite Images

Tamer M. Talal
Dept. of Space
National Authority for Remote Sensing and Space Sciences (NARSS)
Cairo, Egypt
tamer.talal@narss.sci.eg

Fathi E. Abd El-Samie
Dept. of Communications
Faculty of Electronic Engineeing, Menofia University
Menouf, Egypt
fathi_sayed@yahoo.com

Gamal Attiya
Dept. of Computer Science and Engineering
Faculty of Electronic Engineeing, Menofia University
Menouf, Egypt
gamal_mahrouce@yahoo.com

M.I. Dessouky
Dept. of Communications
Faculty of Electronic Engineeing, Menofia University
Menouf, Egypt
dr_moawad@yahoo.com

Mohamed R. Metwalli
Dept. of Data reception
National Authority for Remote Sensing and Space Sciences (NARSS)
Cairo, Egypt
moh_roshdym@yahoo.com

Abstract*—Pan-sharpening considers one of the most important applications for satellite images as it enhances spectral and spatial information for the images. Empirical Mode Decomposition (EMD) is one of the most powerful techniques for pan-sharpening. It first decomposes the image into a set of Intrinsic Mode Functions (IMFs) and a residual component. These panchromatic and multispectral components are then fused to create an enhanced pan-sharpened image. This paper presents an efficient hybrid method for enhancing pan-sharpening of multiband images transmitted from satellite to ground stations. The proposed approach combines this EMD technique with the most powerful conventional method; Discrete Wavelet Transform (DWT), to maximize the pan-sharpening gain. The proposed hybrid method is validated using satellite images of Nile Valley and Suez Canal region, Egypt, captured by Spot-4 and Landsat-8 satellites. The results imply that the proposed hybrid method provides better qualitative and quantitative quality comparing with the individual and the most common pan-sharpening methods.

Keywords*—DWT, EMD, image fusion, Landsat-8, pan-sharpening, and Spot-4.

I. INTRODUCTION

Remote sensing satellites offer a huge quantity of data that has various characteristics of temporal, spatial, radiometric and spectral resolutions. However, several remote sensing applications (such image classification and feature extraction) require high spatial and spectral resolutions at the same time in a single image. Nevertheless, there are constraints to realize this issue by using satellites directly. By satellite imaging, two alternatives of visible images are available; panchromatic and multispectral. The panchromatic images are transmitted with the maximum resolution while the multispectral images are transmitted with coarser/lower resolution. Therefore, for the optimum benefit of these characteristics, the panchromatic image should be combined with the multispectral ones in a single image to convey more information.

Image fusion techniques authorize the integration of different information sources all together to improve information extraction. The main goal is to merge the complementary multi-sensor, multi-temporal and/or multi-view information into one image containing information of greater quality that cannot be achieved otherwise. The exact definition (meaning and measurement) of 'greater quality' relies the dedicated application [1].

Recently, the development of earth remote sensing satellites is mainly directed to enhancing the spatial and spectral information [2]. As the spatial and spectral information are two critical parameters for increasing the image interpretation capability, fusion of spatial and spectral resolution images improves the usage of satellite images. The satellite image fusion of a high spatial resolution panchromatic (PAN) image with the high spectral resolution multispectral (MS) images is called "pan-sharpening" [3].

Several techniques are applied for pan-sharpening such Hue-Saturation-Intensity (IHS), multiplicative (MT), Brovey Transform (BT), High-Pass Filtering (HPF), and Discrete Wavelet Transform (DWT). These techniques may be categorized into some categories. In [4], Schowengerdt classifies them into spectral domain methods, spatial domain methods, and scale space methods. In [5], Ranchin and Wald classifies them into projection-substitution methods, and relative spectral contribution methods. Finally, in [6], Aiazzi and Baronti classifies them into component substitution (CS) methods, relative contribution methods, and Multi-Resolution Analysis (MRA) methods.

Although several techniques are developed, the conventional pan-sharpening techniques can distort the spectral information of the multispectral data while merging. These techniques improve the quality to some extent with spectral distortion. IHS [3], and MT [7], as component substitution methods, provide transcendent visually high-resolution images but don't care about the high-synthesis requirements of spectral information. Therefore, as these methods provide good visual interpretation, high-synthesis of spectral information is important for most remote sensing applications based on spectral signatures [8]. Relative contribution methods such as BT [9], and HPF [10–12] provide better performance in terms of the high-synthesis of spectral information. More recently, the MRA methods such DWT [9] and EMD [13] has been used in image fusion. It was found that multi-sensor pan-sharpening is a tradeoff between the spectral and spatial information as it enhances the spatial resolution by structural injection.

This paper provides an efficient hybrid method for pan-sharpening enhancement of multiband images transmitted from satellite to ground stations. The main idea of the proposals is to hybridize the EMD with the most powerful common fusion methods to emphasize/maximize the pan-sharpening gain. This proposal combines the EMD with the DWT. The proposed method is verified using satellite images of Nile Valley and Suez Canal region, Egypt, captured by Spot-4 and Landsat-8 satellites, respectively. The results imply that the proposed method improve the qualitative and quantitative quality comparing with the conventional methods.

The rest of paper is organized as; Section 2 provides a discussion of the traditional pan-sharpening methods with simple comparison. Section 3 describes the proposed hybrid method while the experimental results and the quality assessments are illustrated in Section 4. Finally, the paper conclusion is included in Section 5.

II. CONVENTIONAL PAN-SHARPENING METHODS

This section presents the most common pan-sharpening techniques including Intensity Hue-Saturation (IHS), Multiplicative Transform (MT), Brovey Transform (BT), High-Pass Filtering (HPF), and Discrete Wavelet Transform (DWT) in addition to Empirical Mode Decomposition (EMD).

A. Intensity-Hue-Saturation

IHS method is a standard pan-sharpening procedure, as a component substitution category, with three MS bands. Originally, it depends on the RGB color space. Meanwhile, it transformed into IHS color space. This color space is often used because the visual human system treats these components as roughly orthogonal axes. Then, the PAN image is histogram matched with the intensity component. After that, the intensity component is replaced with the matched panchromatic image. Finally, the inverse-transform of IHS to RGB is performed. The forward transform of this method is carried out using (1), while the backward transformation is carried out using (2), [3].

$$I = (R + G + B)/3$$

$$S = 1 - (min(R, G, B)/I) \qquad if\ I > 0$$

$$S = 0 \qquad if\ I = 0 \tag{1}$$

$$H = cos^{-1}\left[(R - {}^1\!/_2\, G - {}^1\!/_2\, B)/\sqrt{R^2 + G^2 + B^2 - RG - RB - GB}\right] \quad if\ G \geq B$$

$$H = 360 - cos^{-1}\left[(R - {}^1\!/_2\, G - {}^1\!/_2\, B)/\sqrt{R^2 + G^2 + B^2 - RG - RB - GB}\right] \quad if\ B > G$$

$$R = I + IS * cos(H)/\, cos(60 - H)$$

$$G = I + IS * (1 - cos(H)/\, cos(60 - H)) \tag{2}$$

$$B = I - IS$$

B. Multiplicative Transform

MT combines the two panchromatic/multispectral sets by multiplying each pixel in each MS band by the corresponding pixel of the PAN image [12]. For compensation of the excess brightness values, the square root of the resultant values is applied. The square root of the multiplicative data reduces data to a components that reflects the mixtured spectral properties of the two sets as follows [7]:

$$MLT_{i,j,k} = \sqrt{a \times b \times Pan_{i,j} \times MS_{i,j,k}} \tag{3}$$

where the MLT is the resultant image, *i* and *j* are pixels of band k, Pan and MS are panchromatic and multispectral data respectively. Finally, a and b are weighting coefficients to compensate for the high-brightness effect.

C. Brovey Transform

As a relative contribution category, BT method performs the pan-sharpening by multiplying each MS band by the PAN band, and then dividing each product by the summation of the MS bands as follows [9]:

$$\left.\begin{aligned} R_{Br} &= Pan * R / (R + G + B) \\ G_{Br} &= Pan * G / (R + G + B) \\ B_{Br} &= Pan * B / (R + G + B) \end{aligned}\right\} \tag{4}$$

D. High Pass Filtering

HPF method pertains to the relative contribution category. It performs HP filtering of the PAN image to extract the high frequency components, i.e. spatial details. These components are then injected into the multispectral images to produce the fused image with sharp characteristics [10-12]:

$$Fused_{HPF} = Pan_{hpf} + MS \tag{5}$$

Where: Pan_{hpf} is the PAN image after applying high pass filter.

E. Discrete Wavelet Transform

DWT method is based on MRA that manages the different image resolutions [9]. The DWT breaks down each image into different coefficients containing its information. Therefore, coefficients of PAN and MS images are combined to get a new reconstructed image. The main drawback of this technique is the ringing effects as it discards the low frequency component of the panchromatic image, completely.

F. Empirical Mode Decomposition

EMD is one of the most powerful techniques for pan sharpening. It pertains to the MRA category. This method is similar to the DWT in that it replaces the high frequency components of MS with those that are from PAN. However, the DWT decomposition is related to the predefined wavelet basis while the EMD is a non-parametric data-driven process

that is not required to predetermine the basis during decomposition.

The EMD approach first decomposes a nonlinear and non-stationary signal into a series of Intrinsic Mode Functions (IMFs) and a residual component [14]. They are obtained from the image by a "sifting process" that produces a signal that gets these properties. These components are then fused in a specific way to create an enhanced pan-sharpened image

The EMD method is mainly used for both one dimension (1D) and two dimensions (2D) signal processing. The 1D EMD is used for signal processing. Nevertheless, because pan-sharpening deals with images, 2D EMD is more appropriate.

- One-Dimensional 1D EMD Technique:

The EMD technique was originally developed to decompose one-dimensional 1D signals. Initially, the EMD is used to decompose signals into limited IMFs and a residual component. An IMF can be defined as a function with number of signal extreme points equal to the number of zero crossings or differs by one. The IMFs are got through an iterative process that is called sifting process. The sifting process works as follows [14]:

Step 1: Define the local maximal and minimal points of the input signal $h_{(i,j)}(t)$. Where, i is the IMF number and j is the iteration number, and $h_{(1,1)}(t)$ is the input signal $X(t)$.

Step 2: Evaluate the overhead and down envelopes $u_{(i,j)}(t)$ and $l_{(i,j)}(t)$ by interpolating the local maximal and minimal points using cubic interpolation.

Step 3: Compute the mean envelope $m_{(i,j)}(t)$ using the overhead and down envelopes.

$$m_{(i,j)}(t) = \frac{\left[u_{(i,j)}(t)+l_{(i,j)}(t)\right]}{2} \quad (6)$$

Step 4: Subtract the $h_{(i,j)}(t)$ by the mean envelope to obtain $h_{(i,j+1)}(t)$. If $h_{(i,j+1)}(t)$ satisfies the IMF requirement , then $h_{(i,j+1)}(t)$ is $IMF_i(t)$. Then, subtract the original $X(t)$ by this $IMF_i(t)$ to obtain residual $r_i(t)$. The $r_i(t)$ is considered as the input for next iteration and then repeat Step 1 . If $h_{(i,j+1)}(t)$ does not satisfy the IMF requirement , $h_{(i,j+1)}(t)$ is considered as the input data and then repeat Step 1.

$$h_{(i,j+1)}(t) = h_{(i,j)}(t) - m_{(i,j)}(t) \quad (7)$$

The stopping criterion for sifting process is when the numbers of the zero-crossing and extreme points are the same. The procedure is repeated until the residual $r(t)$ is smaller than a threshold value. Finally, the input signal $X(t)$ can be decomposed into several IMFs and a residual $r_n(t)$ as shown in (8). Equation 8 shows that $X(t)$ can be reconstructed from the IMFs and residual without information loss.

$$X(t) = \sum_{i=1}^{n} IMF_i(t) + r_n(t) \quad (8)$$

- Two-Dimensional 2D EMD Technique:

To apply EMD method to images, 2D EMD is developed based on the original 1D EMD. The process of 2D EMD is performed on rows and then columns. This method determines and interpolates the extreme points in the 2D space. The 2D EMD process is different slightly from 1D EMD as briefly described below [14-16]:

Step 1: Define the local maximal and minimal points of the input image $h_{(i,j)}(p, q)$. Then, perform the cubic interpolation for overhead and down envelopes $ur_{(i,j)}(p, q)$ and $lr_{(i,j)}(p, q)$ along rows and $uc_{(i,j)}(p, q)$ and $lc_{(i,j)}(p, q)$ along columns. Where, i represents the IMF number and j represents the iteration number. Initially, $h_{(1,1)}(p, q)$ is represented by the input image $X(p, q)$.

Step 2: Calculate the mean envelope $m_{(i,j)}(p, q)$ using the overhead and down envelopes along rows and columns, as shown in (9).

$$m_{(i,j)}(p,q) = \frac{\left[ur_{(i,j)}(p,q)+lr_{(i,j)}(p,q)+uc_{(i,j)}(p,q)+lc_{(i,j)}(p,q)\right]}{4} \quad (9)$$

Step 3: Subtract the $h_{(i,j)}(p, q)$ by the mean envelope to obtain $h_{(i,j+1)}(p, q)$, as shown in (10). If $m_{(i,j)}(p, q)$ satisfies the IMF requirement , then $h_{(i,j+1)}(p, q)$ is $IMF_i(p, q)$ and subtract the original signal by this $IMF_i(p, q)$ to get residual $r_i(p, q)$. $r_i(p, q)$ is considered as the input for next iteration and then Step 1 is repeated. If $m_{(i,j)}(p, q)$ does not satisfy the IMF requirement , $h_{(i,j+1)}(p, q)$ is treated as the input data and then Step 1 is repeated.

$$h_{(i,j+1)}(p,q) = h_{(i,j)}(p,q) - m_{(i,j)}(p,q) \quad (10)$$

The stopping criterion for sifting process is when the envelope mean signal is close to zero. The sifting process is repeated until the residual $r(p, q)$ is smaller than a threshold value. Finally, image $X(p, q)$ shall be broken down into several high to low frequency IMFs and a residual $r_n(p, q)$ as illustrated in (11). Equation 11 also demonstrates that the original image can be reconstructed using IMFs and residuals without losing information.

$$X(p,q) = \sum_{i=1}^{n} IMF_i(p,q) + r_n(p,q) \quad (11)$$

III. PROPOSED APPROACH

This section presents an efficient hybrid method for pan-sharpening enhancement of multiband images transmitted from satellite to ground stations. The proposal combines the 2D EMD with the DWT method. Hybrid Method using 2D EMD combined with DWT has been used for another application (classification of images) using support vector machines (SVM) [17].however, hybrid method using 1D EMD with DWT have been used for ECG and EEG signal denoising [18].

A. Hybrid EMD-DWT Method

The hybrid EMD-DWT method compromises the benefits of the 2D EMD and the DWT pan-sharpening techniques. These two techniques belong to the MRA pan-sharpening category. The EMD-DWT hybrid method works as follows.

Step 1: Apply a single level discrete wavelet transform to PAN and the different MS images to extract their approximation and details coefficients matrices.

Step 2: Define the local maximal and minimal components of detail coefficients of the PAN image $pan_{(i,j)}(p_{ch}, q_{ch})$, $pan_{(i,j)}(p_{cv}, q_{cv})$, and $pan_{(i,j)}(p_{cd}, q_{cd})$ and preserve the

approximation coefficient of MS images after its resampling to the PAN image size ca1, ca2, and ca3. Then, perform the cubic spline interpolation for overhead and down envelopes of details coefficients of the PAN image $ur_{(i,j)}(p_{ch}, q_{ch})$ and $lr_{(i,j)}(p_{ch}, q_{ch})$, $ur_{(i,j)}(p_{cv}, q_{cv})$ and $lr_{(i,j)}(p_{cv}, q_{cv})$, and $ur_{(i,j)}(p_{cd}, q_{cd})$ and $lr_{(i,j)}(p_{cd}, q_{cd})$ along rows and $uc_{(i,j)}(p_{ch}, q_{ch})$ and $lc_{(i,j)}(p_{ch}, q_{ch})$, $uc_{(i,j)}(p_{cv}, q_{cv})$ and $lc_{(i,j)}(p_{cv}, q_{cv})$, and $uc_{(i,j)}(p_{cd}, q_{cd})$ and $lc_{(i,j)}(p_{cd}, q_{cd})$ along columns.

Step 3: Calculate the mean envelope $m_{(i,j)}(p_{ch}, q_{ch})$, $m_{(i,j)}(p_{cv}, q_{cv})$, and $m_{(i,j)}(p_{cd}, q_{cd})$ for the PAN details coefficients using the overhead and down envelopes along rows and columns, as shown in (12).

$$m_{(i,j)}(p_{ch}, q_{ch}) = \frac{\begin{bmatrix} ur_{(i,j)}(p_{ch}, q_{ch}) + lr_{(i,j)}(p_{ch}, q_{ch}) \\ +uc_{(i,j)}(p_{ch}, q_{ch}) + lc_{(i,j)}(p_{ch}, q_{ch}) \end{bmatrix}}{4}$$

$$m_{(i,j)}(p_{cv}, q_{cv}) = \frac{\begin{bmatrix} ur_{(i,j)}(p_{cv}, q_{cv}) + lr_{(i,j)}(p_{cv}, q_{cv}) \\ +uc_{(i,j)}(p_{cv}, q_{cv}) + lc_{(i,j)}(p_{cv}, q_{cv}) \end{bmatrix}}{4}$$

$$m_{(i,j)}(p_{cd}, q_{cd}) = \frac{\begin{bmatrix} ur_{(i,j)}(p_{cd}, q_{cd}) + lr_{(i,j)}(p_{cd}, q_{cd}) \\ +uc_{(i,j)}(p_{cd}, q_{cd}) + lc_{(i,j)}(p_{cd}, q_{cd}) \end{bmatrix}}{4} \quad (12)$$

Step 4: Subtract the $pan_{(i,j)}(p_{ch}, q_{ch})$, $pan_{(i,j)}(p_{cv}, q_{cv})$, and $pan_{(i,j)}(p_{cd}, q_{cd})$ by the corresponding mean envelope to obtain $pan_{(i,j+1)}(p_{ch}, q_{ch})$, $pan_{(i,j+1)}(p_{cv}, q_{cv})$, and $pan_{(i,j+1)}(p_{cd}, q_{cd})$ for the PAN details coefficients as shown in (13).

$$pan_{(i,j+1)}(p_{ch}, q_{ch}) = pan_{(i,j)}(p_{ch}, q_{ch}) - m_{(i,j)}(p_{ch}, q_{ch})$$

$$pan_{(i,j+1)}(p_{cv}, q_{cv}) = pan_{(i,j)}(p_{cv}, q_{cv}) - m_{(i,j)}(p_{cv}, q_{cv}) \quad (13)$$

$$pan_{(i,j+1)}(p_{cd}, q_{cd}) = pan_{(i,j)}(p_{cd}, q_{cd}) - m_{(i,j)}(p_{cd}, q_{cd})$$

For the PAN details coefficients, if $m_{(i,j)}(p_{ch}, q_{ch})$, $m_{(i,j)}(p_{cv}, q_{cv})$, and/or $m_{(i,j)}(p_{cd}, q_{cd})$ satisfies the IMF requirement, then $pan_{(i,j+1)}(p_{ch}, q_{ch})$, $pan_{(i,j+1)}(p_{cv}, q_{cv})$, and/or $pan_{(i,j+1)}(p_{cd}, q_{cd})$ is the $IMF_i(p_{ch}, q_{ch})$, $IMF_i(p_{cv}, q_{cv})$, and/or $IMF_i(p_{cd}, q_{cd})$ respectively. Then, subtract the original signal by $IMF_i(p_{ch}, q_{ch})$, $IMF_i(p_{cv}, q_{cv})$, and/or $IMF_i(p_{cd}, q_{cd})$ to get residual $r_i(p_{ch}, q_{ch})$, $r_i(p_{cv}, q_{cv})$, and/or $r_i(p_{cd}, q_{cd})$ that is considered the input for next iteration and then go to Step 2. If $m_{(i,j)}(p_{ch}, q_{ch})$, $m_{(i,j)}(p_{cv}, q_{cv})$, and/or $m_{(i,j)}(p_{cd}, q_{cd})$ does not satisfy the IMF requirement, $h_{(i,j+1)}(p_{ch}, q_{ch})$, $h_{(i,j+1)}(p_{cv}, q_{cv})$, and/or $h_{(i,j+1)}(p_{cd}, q_{cd})$ is treated as the input data and then go to Step 2.

The stopping criterion for sifting process; for PAN details coefficients, is that the envelope mean signal is close to zero or the number of iteration is satisfied. The PAN details coefficient $PAN(p_{ch}, q_{ch})$, $PAN(p_{cv}, q_{cv})$, and $PAN(p_{cd}, q_{cd})$ shall be decomposed into several high to low frequency IMFs and residuals $r_n(p_{ch}, q_{ch})$, $r_n(p_{cv}, q_{cv})$, and $r_n(p_{cd}, q_{cd})$ as illustrated in (14).

$$PAN(p_{ch}, q_{ch}) = \sum_{i=1}^{n} IMF_i(p_{ch}, q_{ch}) + r_n(p_{ch}, q_{ch})$$

$$PAN(p_{cv}, q_{cv}) = \sum_{i=1}^{n} IMF_i(p_{cv}, q_{cv}) + r_n(p_{cv}, q_{cv}) \quad (14)$$

$$PAN(p_{cd}, q_{cd}) = \sum_{i=1}^{n} IMF_i(p_{cd}, q_{cd}) + r_n(p_{cd}, q_{cd})$$

Step 5: After decomposition of details coefficients of the PAN image into their IMFs and a residual and preserving the approximation coefficients of different MS bands, pan-sharpening is performed. Pan-sharpening process is done by reconstructing the fused image using the inverse discrete wavelet transform (IDWT) to the high-frequency IMFs of details coefficients of PAN image with the approximation coefficients of the different MS bands. Then the three reconstructed images are combined to form the pan-sharpened image as (15).

$$X_k(p, q) = IDWT\left(ca_k, IMF_1(p_{ch}, q_{ch}), IMF_1(p_{cv}, q_{cv}), IMF_1(p_{cd}, q_{cd})\right) \quad (15)$$

A simple flowchart for the sequence of execution of the proposed EMD-DWT pan-sharpening process is shown in

Fig. 1. The PAN and different MS images are decomposed first using single level DWT. Then, the sifting process is applied to the details coefficient of the PAN image only while the approximation coefficients of different MS channels are preserved. After that, the high frequency IMFs of the PAN details coefficients are extracted. Finally, applying the single level inverse discrete wavelet transform (IDWT) to that high frequency IMFs and MS approximation coefficients to reconstruct the Pan-sharpened image as shown in

Fig. 1.

IV. PERFORMANCE EVALUATION

In this study, simulations are performed using MATLAB R2013a on windows 10 by an Intel core i5 processor, and 3.0 GB RAMs. The conventional pan-sharpening and the proposed pan-hybrid algorithms are applied to four different image sets. The first image set is of Nile valley of Egypt, captured by the French remote sensing satellite, SPOT-4 that produces images with resolution 10m PAN and 20m MS bands. The second image set is of Suez Canal region, Egypt, captured by the American remote sensing Satellite, Landsat-8 that produces a spatial resolution of 15m and 30m for PAN and MS bands, respectively. The third image set is of Pyramids area, captured by the American remote sensing satellite, QuickBird that produces images with resolution 65cm PAN and 2.6m MS bands. The last image set is of Cairo Stadium region, captured also by the American remote sensing Satellite, Landsat-8.

In each experimental, both the PAN and the MS images are registered. Then, the MS images are resized to match the PAN image size. Finally, the two images are pan-sharpened by using a pan-sharpening method to get a color image with higher spatial resolution. The obtained results are compared

with each other. In this study, several measures for the spectral and spatial distortions are used to assess the pan-sharpening quality for each method. These measures may be categorized as spectral and spatial evaluation criteria.

A. Spectral Evaluation Criteria

The spectral criteria measure the spectral quality of the resultant image through its comparison with the source low resolution MS image. The different spectral evaluation criteria can be described as follows:

- Correlation Coefficient:

The Correlation Coefficient (CC) measures the similarity level between two different images. The CC between each resampled multispectral band and the fused image indicates the spectral compatibility of the fused image. The CC should be as close as possible to 1. The CC value can be calculated by the following formula [19]:

$$cor(x,y) = \frac{\sum_{i=1}^{M}\sum_{j=1}^{N}(x_{i,j} - \bar{x})(y_{i,j} - \bar{y})}{\sqrt{\sum_{i=1}^{M}\sum_{j=1}^{N}(x_{i,j} - \bar{x})^2 (y_{i,j} - \bar{y})^2}} \quad (16)$$

Where, $\bar{x}$, $\bar{y}$ are the mean values of x, y, respectively and x, y are the up-sampled multispectral and the fused images.

- Root Mean Square Error:

The Root Mean Square Error (RMSE) between each resampled multispectral band and the fused image measures the radiance changes of the pixel values. The RMSE is a good indicator for the spectral quality of pan-sharpening, when considered along homogeneity regions in the image. The RMSE has a higher indicator of spectral integrity compared with the CC. The RMSE should be as close as possible to 0. The RMSE can be calculated by the following formula [19]:

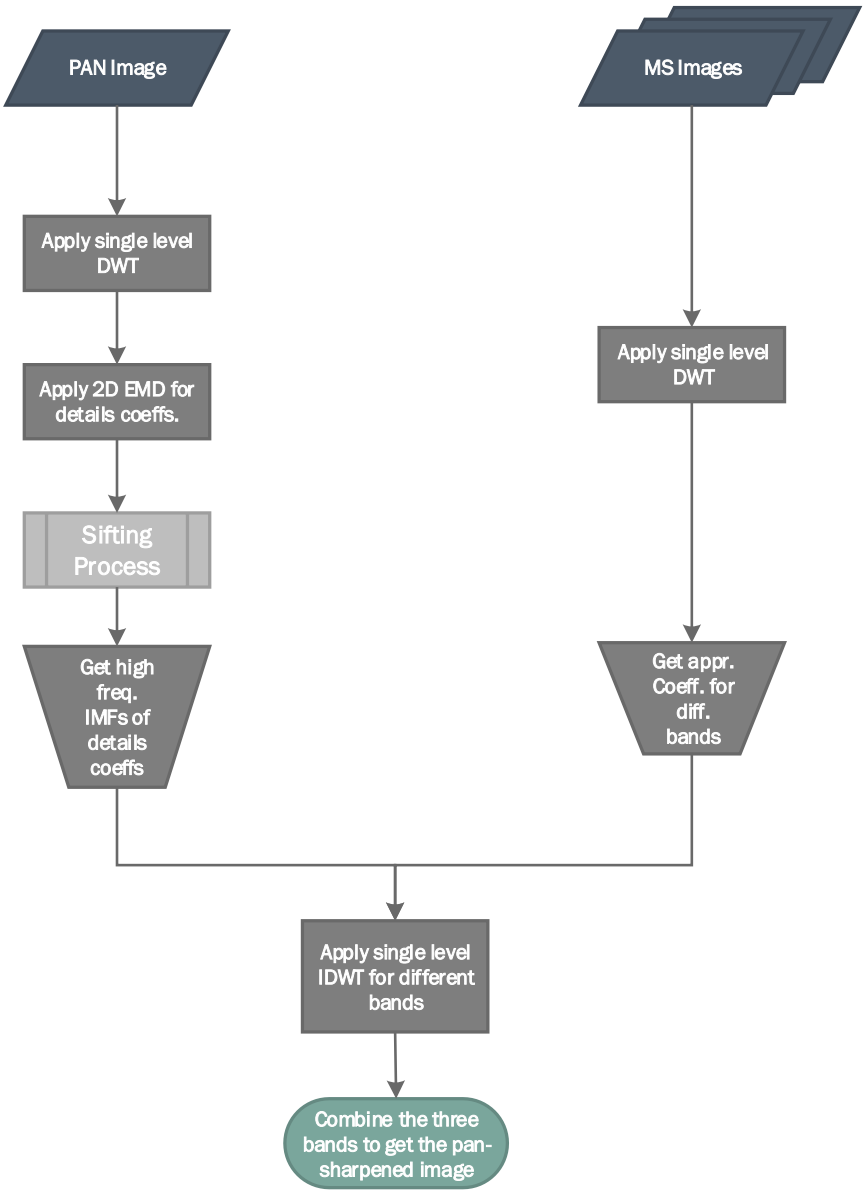

Fig. 1EMD-DWT pan-sharpening block diagram

$$RMSE = \sqrt{E(DN_{ms} - DN_{fused})} \quad (17)$$

Where, DN represents the pixel values, DN_{ms} is a specific band resampled MS image, and DN_{fused} is its corresponding fused image.

- Universal Image Quality Index (UIQI):

Wang and Bovik proposed an excellent parameter, called Universal Image Quality Index (UIQI) to measure the spectral similarity between two images. The UIQI is designed by modeling the spectral distortion as a combination of three components; loss of correlation, radiometric distortion, and contrast distortion that is defined as follows [20]:

$$UIQI = \frac{\sigma_{AB}}{\sigma_A \sigma_B} \cdot \frac{2\mu_A \mu_B}{\mu_A^2 + \mu_B^2} \cdot \frac{2\sigma_A \sigma_B}{\sigma_A^2 + \sigma_B^2} \quad (18)$$

Where, μ_A, μ_B are means of the resampled multispectral and pan-sharpened images A, B, respectively. σ_A, σ_B are the standard deviations of A, B, and σ_{AB} is the covariance between A, B.

The first component is the CC between A and B. The second component measures how close the mean gray levels of A and B are, while the third measures the similarity between the contrasts of A and B. The dynamic range for UIQI is [0-1].

B. Spatial Evaluation Criterion

The Spatial criterion measures the spatial quality of the resultant image through its comparison with the source high resolution PAN image. Evaluating the spatial quality of the pan-sharpened images is more difficult than the spectral one. A few image pan-sharpening scientific papers state the spatial quality indices and there is a little standardization for these indices. The spatial quality is characterized by the edges quality. Thus, the spatial quality indices try to quantify the edge information [21].

- High-Pass Correlation Coefficient (HPCC):

The unique spatial information of the PAN image is mostly concentrated in the high frequency domain. Zhou et al. [21] have used the correlation coefficient between the high-pass filtered fused image and that of the PAN image as a criterion of the spatial quality of the pan-sharpened image. A higher correlation means that more spatial information from the PAN image is incorporated in merging. This means that the spatial information of the pan-sharpened image is high. The Laplacian HPF is the used filter, whose coefficients are given by [22]:

$$\text{Laplacian Coefficients} = \begin{bmatrix} -1 & -1 & -1 \\ -1 & 8 & -1 \\ -1 & -1 & -1 \end{bmatrix}$$

C. Experimental Results and Quality Assessment

As a result of limited size, two satellite image sets only will be displayed for illustration. Fig. 2and Fig. 3 illustrate the obtained results of applying the conventional pan-sharpening methods and the proposed hybrid method for the SPOT-4 French satellite image set of Nile valley, and the Landsat-8 American satellite image set of Suez Canal region, respectively. ForFig. 2, the DWT and EMD-DWT methods preserve the most of spectral information of the original MS image by visual inspection, and also preserve the most spectral information of the original MS image for Fig. 3.

Error! Reference source not found. and **Error! Reference source not found.** give a simple comparison among different pan-sharpening techniques for the two illustrated satellite image sets. For SPOT-4 image set, the EMD-DWT hybrid technique enforces the best spectral quality, while EMD method enforces the highest spatial quality as shown in **Error! Reference source not found.** that ensures importance of the hybrid technique compared to EMD. Also, EMD-DWT hybrid technique decreases the computational time of EMD technique noticeably, as shown in **Error! Reference source not found.**. This is because it applies the EMD technique to the approximated and detail components of the PAN and MS images not to the whole images. For Landsat-8 image set, the EMD-DWT hybrid technique enforces the best spectral quality as shown in Table 2. This is because the DWT extracts the approximation (the most spectral) information of the multispectral images and fuse it into the first high frequency IMF components of the panchromatic detail coefficients. While, EMD method enforces better spatial quality than most of conventional methods except HPF and that ensures the importance of hybrid with EMD as it enhances the spectral quality while preserving little bit the spatial information with enhancement of computational time than EMD technique.

These results imply that the proposed hybrid technique enhances the pan-sharpening quality for different satellite images as it preserves little bit the spatial quality of images.

Fig. 4 shows the different quality indices for the different pan-sharpening techniques. The different quality indices are calculated for the four satellite image sets of pyramids, Nile Valley, Suez Canal region, and Cairo Stadium region, Egypt, captured by Quickbird, Spot-4 and Landsat-8 satellites. This estimation provides the impact of different image objects to the selection of pan-sharpening technique, as they are object-wise techniques. The execution time of the proposed technique using EMD-DWT is less than using EMD only due to decreasing the dimension of the processed images as applying the EMD to individual coefficients as indicated in

Fig. 1.

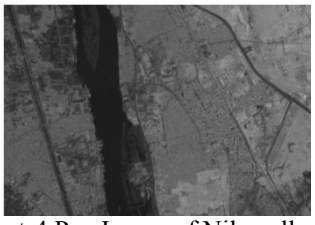

a) Spot-4 Pan Image of Nile valley (10 m resolution)

b) Spot-4 Multispectral Image of Nile Valley (20 m resolution)

c) Brovey method [8]

d) IHS method [2]

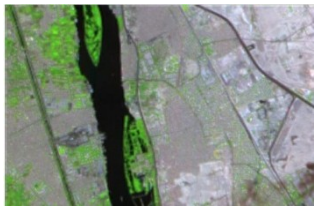

e) HPF method [9]-[13]

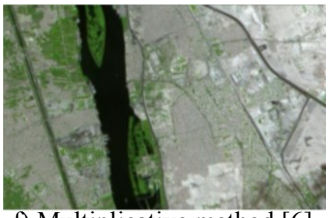

f) Multiplicative method [6]

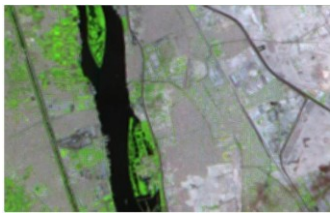

g) DWT method [8]

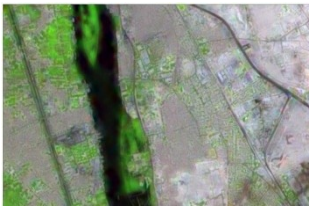

h) EMD method [14]

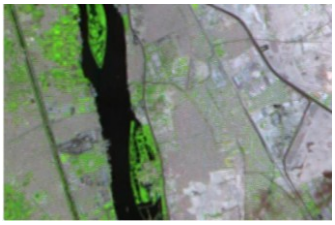

i) EMD_DWT method

Fig. 2Results of applying different pan-sharpening methods for SPOT-4 French satellite image of Nile Valley

a) Landsat-8 Pan Image of Suez Canal area (15 m resolution)

b) Landsat-8 Multispectral Image of Suez Canal area (30 m resolution)

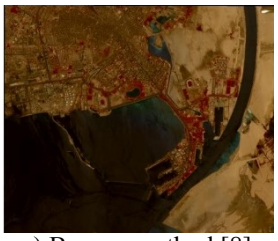

c) Brovey method [8]

d) IHS method [2]

e) HPF method [9]-[13]

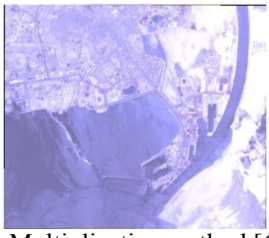

f) Multiplicative method [6]

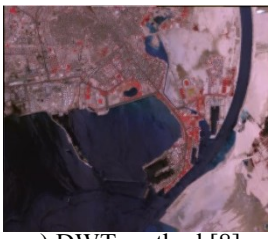

g) DWT method [8]

h) EMD method [14]

i) EMD_DWT method

Fig. 3 Results of applying different pan-sharpening methods to Landsat-8 American satellite image

TABLE 1QUALITY ASSESSMENT RESULTS FOR SPOT-4 SATELLITE IMAGE

Pan-sharpening Technique	Spectral Quality			Spatial Quality	Execution Time (s)
	Correlation Coefficient (CC)	*Root Mean Square Error (RMSE)*	*Universal Image Quality Index (UIQI)*	*High Pass Correlation Coefficient (HPCC)*	
Brovey	0.9532	0.0379	0.9432	0.8955	1.1003
HPF	0.9891	0.0116	0.9885	0.9046	0.8424
HIS	0.9740	0.0158	0.9739	0.8973	0.5108
Multiplicative	0.9751	0.0276	0.9699	0.9118	0.2439
DWT	0.9921	0.0087	0.9921	0.7573	0.5612
EMD	0.9639	0.0186	0.9639	**0.9138**	488.4665
EMD_DWT	**0.9956**	**0.0065**	**0.9956**	0.7633	**147.1155**

TABLE 2QUALITY ASSESSMENT RESULTS FOR LANDSAT-8 SATELLITE IMAGE

Pan-sharpening Technique	Spectral Quality			Spatial Quality	Execution Time (s)
	Correlation Coefficient (CC)	*Root Mean Square Error (RMSE)*	*Universal Image Quality Index (UIQI)*	*High Pass Correlation Coefficient (HPCC)*	
Brovey	0.9040	12.7169	0.6214	0.7817	1.7311
HPF	0.9880	1.5180	0.9875	**0.8013**	0.1510
IHS	0.7809	5.0001	0.7803	0.5042	0.9678
Multiplicative	0.9123	46.1768	0.7522	0.7674	0.4029
DWT	0.9918	1.3671	0.9917	0.6366	0.9918
EMD	0.9142	3.8530	0.9132	0.7982	631.4797
EMD_DWT	**0.9966**	**0.8278**	**0.9966**	0.3726	**181.5818**

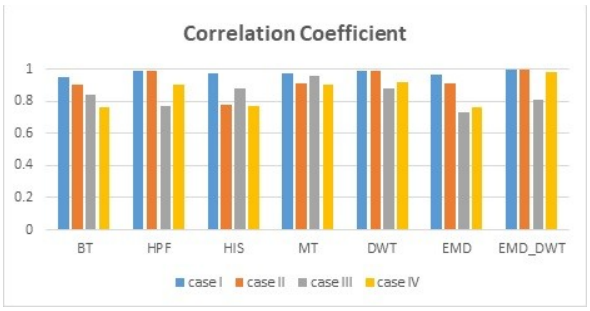

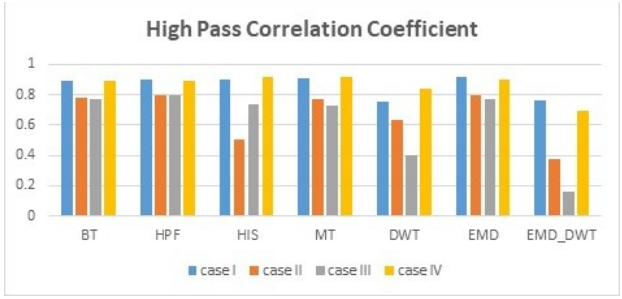

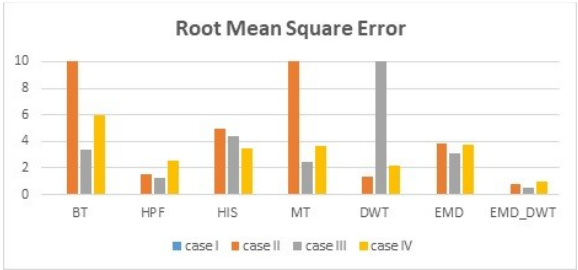

Fig. 4 Quality indices estimation for different satellite images

CONCLUSION

In this paper, an efficient hybrid technique for enhancing pan-sharpening of multiband images transmitted from satellite to ground stations are presented, implemented, and evaluated. The hybrid proposal combines the Empirical Mode Decomposition (EMD) with the Discrete Wavelet Transform (DWT). The proposed method is evaluated using satellite image sets of pyramids, Cairo and Suez Canal region, Egypt, captured by Quickbird, Spot-4, and Landsat-8 satellites, respectively. The experimental results implied that the proposed method enhances the pan-sharpening spectrally and somehow spatially. The EMD-DWT hybrid method is noticeable superior among the conventional pan-sharpening methods as it preserves the spatial quality of images and has less computational time than using EMD only.

ACKNOWLEDGMENT

The authors would like to thank the NARSS organization as it provided the SPOT-4 and Landsat-8 satellite images, and all colleagues in the NARSS who supported in this work.

REFERENCES

[1] L. Wald, “Some terms of reference in data fusion,” IEEE Trans. on Geoscience and Remote Sensing, vol. 37, no. 3, pp. 1190–1193, May 1999.

[2] Z. Wang, D. Ziou, C. Armenakis, D. Li, and Q. Li, “A comparative analysis of image fusion methods” IEEE Trans. on Geoscience and Remote Sensing, vol. 43, no. 6, pp. 1391–1402, June 2005.

[3] Z Li, J Chen, E Baltsavias, “Advances in Photogrammetry”, Remote Sensing and Spatial Information Sciences: ISPRS Congress Book, Taylar & Francis Group, 2008.

[4] R. A. Schowengerdt, “Remote Sensing: Models and Methods for Image Processing”, 2nd edition Orlando, FL: Academic, 1997.

[5] T. Ranchin and L. Wald, “Fusion of high spatial and spectral resolution images: The ARSIS concept and its implementation,” Photogrammetry Engineering Remote Sensing, vol. 66, no. 1, pp. 49–61, 2000.

[6] B. Aiazzi, S. Baronti, and M. Selva, “Improving component substitution pan-sharpening through multivariate regression of MS+Pan Data”, IEEE Trans. on Geoscience and Remote Sensing, vol. 45, no. 10, October 2007.

[7] S. S. Han, H. T. Li, and H. Y. Gu, “The study on image fusion for high spatial resolution remote sensing images”, The International Archives of the Photogrammetry, Remote Sensing and Spatial Information Sciences. vol. XXXVII. part B7, pp. 1159–1164, Beijing, 2008.

[8] J. G. Liu, “Smoothing filter-based intensity modulation: A spectral preserve image fusion technique for improving spatial details,” Journal of Remote Sensing, vol. 21, no. 18, pp. 3461–3472, 2000.

[9] H. Liu, and X. Zhang, “Comparison of data fusion techniques for Beijing-1 micro-satellite images”, Urban Remote Sensing Joint Event, IEEE, 2009.

[10] S.de Béthune, F. Muller, and J. P. Donnay, “Fusion of multi-spectral and panchromatic images by local mean and variance matching filtering techniques,” Fusion of Earth Data Conf., Jan. 28–30, 1998.

[11] B. Aiazzi, L. Alparone, S. Baronti, and A. Garzelli, “Context-driven fusion of high spatial and spectral resolution images based on oversampled multi-resolution analysis,” IEEE Trans. On Geoscience Remote Sensing, vol. 40, no. 10, pp. 2300–2312, Oct. 2002.

[12] H. Ghassemian, “A review of remote sensing image fusion methods”, Journal of Information Fusion, Vol. 32, Part A, pp. 75-89, Nov. 2016.

[13] H. Hariharan, A. Gribok, M. Abidi, and A. Koschan, "Image Fusion and Enhancement via Empirical Mode Decomposition," Journal of Pattern Recognition Research, vol. 1, no. 1, pp. 16-32, January 2006.

[14] T. A. Teo and C. C. Lau,” Pyramid-Based Image Empirical Mode Decomposition for the Fusion of Multispectral and Panchromatic Images”, EURASIP Journal on Advances in Signal Processing, 2012.

[15] S. Chen, y. Su, R. Zhang, and J. Tian, “ Fusing Remote Sensing Images using a Trous Wavelet Transform and Empirical Mode Decomposition.”, Pattern Recognition Letter, vol.29, 330–342, 2008.

[16] B. Demir, S. Ertürk and M. K. Güllü, " Empirical Mode Decomposition of Hyperspectral Images for Support Vector Machine Classification, " IEEE Trans. On Geoscience and Remote Sensing letters, Vol. 8, No. 2, pp. 4071-4084, March. 2011.

[17] E. T. Gormas, N. Canagaraiah and A. Achim," Dimensionality Reduction of Hyperspectral images using Empirical Mode Decomposition and Wavelets, " IEEE Journal of Selected Topics in Applied Earth observations and Remote sensing, Vol. 5, No. 6, pp. 1821-1830, Dec. 2012.

[18] S. Lahmiri and M. Boukadoum, "A Weighted Bio-signal Denoising Approach Using Empirical Mode Decomposition," Biomed. Eng.Letter , Vol.5, pp. 131-139, 2015.

[19] M. R. Metwalli. , “Assessing the quality of satellite images using advanced data fusion techniques”, Ph.D. thesis in Electronic Engineering, Menofia University, Egypt, 2012.

[20] Z. Wang, and A. C. Bovik, “A Universal Image Quality Index," IEEE Signal Processing Letter, vol. 9, no. 3, pp. 81-84, 2002.

[21] P. S. Pradhan, R. L. King, N. H. Younan, and D. W. Holcomb, “Estimation of The Number of Decomposition Levels for a Wavelet-Based Multiresolution Multisensor Image Fusion," IEEE Transactions on Geoscience and Remote Sensing, Vol. 44, No. 12, pp. 3674-3686, 2006.

[22] J. Zhou, D.L. Civco, and J.A. Silander, “A wavelet transform method to merge Landsat TM and SPOT panchromatic data,” International Journal of Remote Sensing, vol.19, no.4, pp.743-757, 1998.